Published in final edited form as:
ACS Med Chem Lett. ; 3(9): 721–725. doi:10.1021/ml300129b.

From *in Silico* Discovery to *intra*-Cellular Activity: Targeting JNK-Protein Interactions with Small Molecules

Tamer S. Kaoud[a,b,¶], **Chunli Yan**[f,¶], **Shreya Mitra**[g], **Chun-Chia Tseng**[a], **Jiney Jose**[a,g], **Juliana M. Taliaferro**[a,b], **Maidina Tuohetahuntila**[a], **Ashwini Devkota**[a,e], **Rachel Sammons**[c,f], **Jihyun Park**[a,d], **Heekwang Park**[h], **Yue Shi**[c,f], **Jiyong Hong**[h], **Pengyu Ren**[c,f], and **Kevin N. Dalby**[a,b,c,d,e]

[a]Division of Medicinal Chemistry, The University of Texas MD Anderson Cancer Center, Houston, TX 77030

[b]Graduate Programs in Pharmacy, The University of Texas MD Anderson Cancer Center, Houston, TX 77030

[c]Biomedical Engineering, The University of Texas MD Anderson Cancer Center, Houston, TX 77030

[d]Cell and Molecular biology, The University of Texas MD Anderson Cancer Center, Houston, TX 77030

[e]Texas Institute for Drug and Diagnostic Development, The University of Texas MD Anderson Cancer Center, Houston, TX 77030

[f]Department of Biomedical Engineering, The University of Texas MD Anderson Cancer Center, Houston, TX 77030

[g]The University of Texas MD Anderson Cancer Center, Houston, TX 77030

[h]Department of Chemistry, Duke University, Durham, NC 27708, USA

Abstract

The JNK-JIP1 interaction represents an attractive target for the selective inhibition of JNK-mediated signaling. We report a virtual screening (VS) workflow, based on a combination of three-dimensional shape and electrostatic similarity to discover novel scaffolds for the development of non-ATP competitive inhibitors of JNK targeting the JNK-JIP interaction. Of 352 (0.13%) compounds selected from the NCI diversity set more than 22% registered as hits in a biochemical kinase assay. Several compounds discovered to inhibit JNK activity under standard kinase assay conditions also impeded JNK activity in HEK293 cells. These studies led to the discovery that the lignan (−)-zuonin A inhibits JNK-protein interactions with a selectivity of 100-fold over ERK2 and p38 MAPKα. These results demonstrate the utility of a virtual screening protocol to identify novel scaffolds for highly selective, cell-permeable inhibitors of JNK-protein interactions.

Correspondence to: Pengyu Ren; Kevin N. Dalby.

¶***Author Contributions***
These authors contributed equally.

Present Addresses
107 West Dean Keaton, BME, The University of Texas at Austin, TX 78712, USA. E mail: kinases@me.com or pren@mail.utexas.edu

Supporting Information: Calculated Binding Free Energies (kcal mol^{-1}) of BI-78D3 in Complex with JNK1, NCI IDs of the compounds, ROCS and EON scores of the compounds, further characterization of the 11 hits, detailed computational and experimental methods. This material is available free of charge via the Internet at http://pubs.acs.org.

Keywords

virtual screening; JNK; non-ATP competitive inhibitor; JIP-JNK interaction; molecular docking and dynamics

c-Jun *N*-terminal kinases (JNKs) belong to the mitogen activated protein kinase (MAPK) family and are encoded by three genes (*Jnk1*, *Jnk2*, and *Jnk3*), which produce at least 10 different spliceforms. JNK1 and JNK2 show a broad tissue distribution, whereas JNK3 expression is more restrictive.[1] JNK1–3 are activated by extracellular stimuli, such as stress or cytokines, which leads to the phosphorylation of several cellular substrates implicated in cell survival and proliferation.[2]

The JNK signaling pathway is associated with the pathogenesis of several diseases, including, diabetes, cancer, and neurological diseases.[3] Most drug discovery efforts have focused on the development of ATP-competitive inhibitors of JNK,[4] which presents challenges due to the high level of homology in the ATP-binding site amongst protein kinases.[5]

An alternative strategy to develop a specific JNK inhibitor is to target a substrate recruitment site. Inhibitors that target the protein-protein interaction sites of MAPK kinases are expected to exhibit pharmacological profiles that are quite distinct from those that bind within the active site. Although the development of small molecules targeting protein-protein interactions represents a challenging area, progress has been made with a variety of approaches.[5] Scaffolding proteins, such as the JNK Interacting Proteins (JIP 1–4)[6] and arrestin[7] are known to bind JNK to enhance its activation *in vivo*. Several non-ATP competitive inhibitors of JNK target the JIP-JNK interaction. For example, JIP-based peptide inhibitors that correspond to the D-site of JIP1 bind the D-recruitment site (DRS) of JNK and act as specific inhibitors of JNK-ligand interactions.[8] Recently, we engineered potent (IC_{50} ~90 nM) JIP-based peptide inhibitors with demonstrated specificity for the JNK2-isoform.[9] In 2008, Stebbins et al. identified the thiadiazole BI-78D3 (Figure 1A) as a small molecule targeting the JNK-JIP interaction.[10] BI-78D3 was identified as a non-ATP competitive inhibitor of JNK. Several analogs of BI-78D3 with improved plasma stability have been reported.[11] There have also been efforts to discover different scaffolds that act as non-ATP inhibitors of JNK.[12]

In this work, we used Shape-Based Virtual Screening (VS) to discover JNK-selective inhibitors that do not compete with ATP. The starting point for this virtual screen was BI-78D3 (Figure 1A). Ligand-based virtual screening with BI-78D3 as the query molecule was applied to search the (National Cancer Institute) NCI Diversity Set[13] for selective inhibitors. The evaluation of selected compounds resulted not only in new scaffolds for the development of potential therapeutic agents that target the JNK-JIP interaction, but also yielded the discovery that the lignan (−)-zuonin A inhibits JNK-protein interactions with a selectivity of 100-fold over ERK2 and p38 MAPKα.

Generation of a Bioactive Conformation for the Query Ligand BI-78D3

BI-78D3 (Figure 1A) is known to displace pepJIP1 from JNK.[10] To gain insight into its potential bioactive conformations when bound to JNK1, we constructed a model of the protein-ligand complex using coordinates from the X-ray crystal structure of the JNK1•pepJIP1 complex[8] (Figure 1B and 1C), where pepJIP1 binds the D-recruiting site (DRS) of JNK. We searched the surface of JNK1, centering on the DRS in order to construct a model for BI-78D3 bound to JNK1 using molecular docking. Three possible docking sites were identified (Figure 1D), including five potential poses (binding structures) at site 2,

which is situated in between a negatively charged surface, Φ_{chg}, and a hydrophobic pocket, Φ_{hyd}, and further defined by β8, αE, loop 16 and αD (Figure 1E). The poses at site 2 were used as starting structures for further molecular dynamics simulations (MD) to determine the dynamically stable protein-ligand binding modes. These were then further interrogated by MM-PBSA (molecular mechanics/Poisson–Boltzmann (PB) solvent-accessible surface area methodology)[14] to estimate their relative binding free energy. The estimated binding free energy ΔG_b of pose 5 was slightly more favored (Table S1). Interestingly, after 3 ns of MD simulation, pose 5 re-oriented to place the nitro group of BI-78D3 in the proximity of Glu-126 and Arg-127 (*α*E) (Figure 1E). Accordingly, the ligand conformer in this new pose was used as the bioactive conformation of BI-78D3 with which to carry out the virtual screen. It should be noted that Stebbins et. al[10] proposed an alternative binding mode with the benzodioxan moiety of BI-78D3 occupying the hydrophobic (Φ_{hyd}) region that corresponds to the highly conserved leucines of pepJIP1 (Figure 1C). This binding mode was not identified in our studies.

Combined shape and charge-based virtual screening

A schematic summary of the overall virtual screening procedure utilized in this study is presented in Figure 1F. The library used in the ligand-based virtual screening is the NCI Diversity Set, which contains 260,071 compounds.[13] Each compound was expanded into a set of twenty three-dimensional conformations using Omega 2.3.2 of OpenEye software. The three-dimensional shape comparison between BI-78D3 and the molecules in the NCI Diversity Set was performed using ROCS 2.3.1. The top 1000 ranked compounds from the shape-based screen were then assessed for similarity to BI-78D3 using EON 2.0.1, which calculates an Electrostatic Tanimoto (ET) score which is a measure of the electrostatic similarity between two small molecules.[15] A total of 750 compounds, representing the merging of the top 500 hits from the two screens were subsequently selected for further biochemical screening using *in vitro* kinase assays (Table S2).

Assessment of enrichment for targeting JNK

352 of the top 750 compounds were available from NCI. An enrichment experiment was performed to compare these compounds to 350 selected randomly from the same library. The % inhibition of both the *in silico* VS-selected and randomly selected compounds (at 10 μM concentrations) towards JNK1 and Trpm7 (an atypical kinase) was determined using an *in vitro* kinase assay. While 80 of 350 compounds from the *in silico* analysis were identified as hits when screened at 10 μM against JNK1 (greater than 25% inhibition above a DMSO control) none of the randomly selected (JNK1 control) compounds inhibited JNK1 by more than 20% (Figure 2A). Trpm7, which has little sequence similarity to JNK,[16] exhibited limited inhibition when treated with either the VS-selected compounds, or the random set (Figure 2A). Surprisingly, when assayed against substrates that target the DRS, the MAP kinases ERK2 and p38MAPKα showed broadly similar results to Trpm7 and eEF-2K (Figure 2B). Together, these results validate the VS protocol as a useful tool for the identification of inhibitors that target JNK1.

Prioritizing hits and potential mechanisms of protein interference agents targeting the DRS of JNK

The virtual screening strategy we followed in this work is predicted to discover inhibitors that compete with JIP and c-Jun at the DRS of JNK. We decided to examine several promising hits (compounds **1** – **11**) in more detail (Figure 3A), and prepared authentic samples of both enantiomers of compound **2**, **2**$^{(-)}$ and **2**$^{(+)}$.[i] As would be expected, compounds **1** – **11** exhibit structural features similar to those found in BI-78D3, including

either a benzo[d][1,3]dioxole moiety (compounds, **1**, **2**, **5**, **6**, and **8**), an aromatic ring containing an electronegative substituent (compounds **3**, **4**, **7**, **10** and **11**), or a nitro group (compounds **7**, and **9**). Figures 3B and 3C show the structural overlaps and electrostatic distribution, respectively of several of the hits identified in the screen.

We performed dose-response curves, on the HPLC-purified compounds, examining their ability to inhibit c-Jun phosphorylation by JNK2 in an in vitro kinase assay (Table 1). The inhibition profile for JNK1 and JNK2 were similar (Figure 2B) enabling us to use either JNK1 or JNK2 in the subsequent biochemical characterization of the compounds. As an additional biochemical screen we developed a FITC-JIP peptide displacement assay to estimate the ability of compounds to displace JIP from JNK (Table 1). By using these two screens compounds were assessed for their ability to inhibit the binding of two different D-site sequences to JNK.

IC_{50} values for the inhibition of JNK, or the displacement of JIP by the hits ranged from 0.7 to 22 μM and from 2.2 to 41 μM, respectively (Table 1). The maximal inhibition of JNK1 in the kinase assay at saturating inhibitor ranged from 30 to 100% and the maximal displacement of JIP in the binding assay ranged from 25 to 100%. In general, the two assays correlate quite well. However, some compounds appeared to perform slightly better in one assay compared to the other, which is not surprising given that the assays utilize different D-sites and experimental conditions. Compound **1** is the highest ranked compound by EON due to its electrostatic similarity to BI-78D3. It fully (100%) inhibits JNK2 at saturating concentrations exhibiting an IC_{50} value of 0.7 ± 0.1 μM (Figure 2C). As we expected it to be a Redox Cycling Compound (RCC), due to the presence of a pyrimidotriazinedione cluster, it was assessed in the presence of 100 U/mL of catalase. However, catalase had no effect on its activity (supporting information).[17] Unfortunately, its fluorescence spectrum precluded an assessment using the displacement assay. As predicted by the virtual screen, $\mathbf{2}^{+}$ ((+)-zuonin A)[i] binds JNK1, displaying an IC_{50} of 2.6 ± 0.2 μM, however it exhibits only 15% inhibition at saturation (Table 1). In contrast, its enantiomer $\mathbf{2}^{(-)}$, (−)-zuonin A, exhibits a more pronounced 80% inhibition at saturation in both assays (Figures 2C and S1), with a similar IC_{50}. These data suggest that upon binding, $\mathbf{2}^{(-)}$ blocks the binding of the D-sites to JNK more effectively than $\mathbf{2}^{(+)}$. At saturation compound **3** exhibits 100% inhibition in both assays, although it is 3-fold more effective in the kinase assay (IC_{50} of 14 ± 1.3 μM) compared to the displacement assay (IC_{50} of 58 ± 6 μM) (Figure S1). Compound **4** performs equally in both assays (IC_{50} of 21 and 41 μM respectively, ~ 80 % max). Compounds **5, 6, 8** and **10** exhibit maximal inhibitions of less than 50% in both assays. Compounds **7** and **9** inhibit c-Jun phosphorylation, but do not displace labeled JIP peptide from JNK2. The potency of compound **11** was significantly diminished by 0.01% Triton X-100 (Figure S2), suggesting that its inhibition may be due to non-specific binding or aggregation (Supporting information).

To assess the nature of their interactions with JNK we docked compounds **1**, $\mathbf{2}^{(-)}$, **3** and **4** onto the DRS of JNK1 (Figure S3). The results of this analysis support the notion that all four compounds bind site 2. A molecular dynamics (MD) analysis, further suggest that the presence of a planar ring in proximity to the two aromatic rings of Tyr-130 and Trp-324, forms potentially favorable **π-π** stacking interactions, however it is clear that the orientations of the ring are predicted to vary significantly, suggesting that some compounds may form stronger interactions at this locus than others (Figures 1E and S3). Differences in the binding modes for each compound could account for the variability in the maximal

[i]We report elsewhere (Kaoud, T.S. et. al, submitted) that 2^{+}, 5,5′-(2*R*,3*R*,4*S*,5*R*)-3,4-dimethyltetrahydrofuran-2,5-diyl)bis(benzo[*d*][1,3]dioxole) corresponds to the natural product (+)-zuonin A, while $2^{(-)}$,5,5′-((2*S*,3*R*,4*S*,5*S*)-3,4-dimethyltetrahydrofuran-2,5-diyl)bis(benzo[*d*][1,3]dioxole), corresponds to (−)-zuonin A.

inhibition achieved at saturation (Figure S3). This is an important consideration for the future development of analogs.

Selectivity of the hits

To profile the selectivity of the hits towards JNK, the IC_{50} of each compound was determined against ERK2 and p38MAPKα (Figure S4) and (Table 1). Several compounds exhibited selectivity for JNK. Most notably, **2**$^{(-)}$ exhibits 100-fold selectivity for JNK2 over both ERK2 and p38MAPKα. Several other compounds **5**–**7**, **9** and **10**, while less potent inhibitors of JNK were also selective and in fact exhibited no significant inhibition of ERK2 or p38MAPKα. Compound **1** exhibited little selectivity between the MAPKs, while compounds **3** and **8**, inhibited both JNK and ERK2, and compound **4** preferred ERK2 and p38. The selectivity profile of these compounds strongly demonstrates the ability of the virtual screening protocol to identify molecules that target specific sites in JNK with acceptable selectivity.

Cellular Activity

Compounds such as **2**$^{(-)}$ have potential to inhibit JNK signaling by compromising protein interactions with the DRS. The ability of the hits to inhibit JNK in HEK293 cells was therefore examined. The ability of each compound to inhibit the phosphorylation of JNK and c-Jun (a substrate of the JNKs,[18]) was tested following stimulation of JNK by anisomycin[9a] and visualized through western blot analysis (Figure 4 & S5). As expected, several compounds showed inhibition of JNK and c-Jun phosphorylation in HEK293 cells (e.g. **1**, **2**$^{(-)}$ and **6**).

In conclusion

the NCI diversity set, consisting of approximately 260 thousand compounds, was virtually screened against the protein-binding site of JNK. A total of 11 small molecules were identified as potential inhibitors of JIP-JNK binding. (−)-zuonin A showed marked selectivity for JNK over other MAPKs. Several of the inhibitors described here represent starting points for the development of potent and selective small molecules capable of compromising the binding of proteins to the DRS of JNK.

Supplementary Material

Refer to Web version on PubMed Central for supplementary material.

Acknowledgments

Funding Sources

The authors declare no competing financial interest.

This research was supported in part by the grants from the Welch Foundation (F-1390), CPRIT (RP110539, RP101501), and NIH (R01GM059802, R01GM079686). Support from the Texas Advanced Computing Center (TACC) and TeraGrid (MCB100057) and The A.D. Hutchinson Student Endowment Fellowship (to TSK) are acknowledged. The Authors thank Dr. Philip LoGrasso for providing JNK plasmids and Dr. Eric V. Anslyn for providing laboratory space to JJ. Dr. Angel Syrett prepared the TOC figure.

ABBREVIATIONS

JNK c-Jun N-terminal kinases

MAPK	mitogen activated protein kinase
DRS	D-recruitment site
NCI	National Cancer Institute
VS	virtual screening
MD	molecular dynamics
DELFIA	Dissociation Enhanced Lathanide Fluoro-Immuno Assay
Trpm7	the kinase domain of human Trpm7 channel-kinase, containing the last 462 amino acids (1403–1864) of Trpm7/ChaK1 (GenBank accession number AF346629)
eEF2K	full length eukaryotic elongation factor 2 kinase

References

1. Barr RK, Bogoyevitch MA. The c-Jun N-terminal protein kinase family of mitogen-activated protein kinases (JNK MAPKs). Int J Biochem Cell B. 2001; 33(11):1047–1063.
2. (a) Kyriakis JM, Avruch J. Mammalian mitogen-activated protein kinase signal transduction pathways activated by stress and inflammation. Physiol Rev. 2001; 81(2):807–869. [PubMed: 11274345] (b) Pearson G, Robinson F, Gibson TB, Xu BE, Karandikar M, Berman K, Cobb MH. Mitogen-activated protein (MAP) kinase pathways: Regulation and physiological functions. Endocr Rev. 2001; 22(2):153–183. [PubMed: 11294822]
3. (a) Manning AM, Davis RJ. Targeting JNK for therapeutic benefit: From JuNK to gold? Nat Rev Drug Discov. 2003; 2(7):554–565. [PubMed: 12815381] (b) Bogoyevitch MA. Therapeutic promise of JNK ATP-noncompetitive inhibitors. Trends Mol Med. 2005; 11(5):232–239. [PubMed: 15882611]
4. Siddiqui MA, Reddy PA. Small molecule JNK (c-Jun N-terminal kinase) inhibitors. J Med Chem. 2010; 53(8):3005–12. [PubMed: 20146479]
5. Schnieders MJ, Kaoud TS, Yan C, Dalby KN, Ren P. Computational Insights for the Discovery of Non-ATP Competitive Inhibitors of MAP Kinases. Curr Pharm Des. 2012
6. Yasuda J, Whitmarsh AJ, Cavanagh J, Sharma M, Davis RJ. The JIP group of mitogen-activated protein kinase scaffold proteins. Mol Cell Biol. 1999; 19(10):7245–54. [PubMed: 10490659]
7. Zhan X, Kaoud TS, Dalby KN, Gurevich VV. Nonvisual arrestins function as simple scaffolds assembling the MKK4-JNK3alpha2 signaling complex. Biochemistry. 2011; 50(48):10520–9. [PubMed: 22047447]
8. Heo JS, Kim SK, Seo CI, Kim YK, Sung BJ, Lee HS, Lee JI, Park SY, Kim JH, Hwang KY, Hyun YL, Jeon YH, Ro S, Cho JM, Lee TG, Yang CH. Structural basis for the selective inhibition of JNK1 by the scaffolding protein JIP1 and SP600125. Embo J. 2004; 23(11):2185–2195. [PubMed: 15141161]
9. (a) Kaoud TS, Mitra S, Lee S, Taliaferro J, Cantrell M, Linse KD, Van Den Berg CL, Dalby KN. Development of JNK2-selective peptide inhibitors that inhibit breast cancer cell migration. ACS chemical biology. 2011; 6(6):658–66. [PubMed: 21438496] (b) Mitra S, Lee JS, Cantrell M, Van den Berg CL. c-Jun N-terminal kinase 2 (JNK2) enhances cell migration through epidermal growth factor substrate 8 (EPS8). J Biol Chem. 2011; 286(17):15287–97. [PubMed: 21357683]
10. Stebbins JL, De SK, Machleidt T, Becattini B, Vazquez J, Kuntzen C, Chen LH, Cellitti JF, Riel-Mehan M, Emdadi A, Solinas G, Karin M, Pellecchia M. Identification of a new JNK inhibitor targeting the JNK-JIP interaction site. Proceedings of the National Academy of Sciences of the United States of America. 2008; 105(43):16809–13. [PubMed: 18922779]
11. (a) De SK, Chen LH, Stebbins JL, Machleidt T, Riel-Mehan M, Dahl R, Chen V, Yuan H, Barile E, Emdadi A, Murphy R, Pellecchia M. Discovery of 2-(5-nitrothiazol-2-ylthio)benzo[d]thiazoles as novel c-Jun N-terminal kinase inhibitors. Bioorganic & Medicinal Chemistry. 2009; 17(7): 2712–7. [PubMed: 19282190] (b) De SK, Stebbins JL, Chen LH, Riel-Mehan M, Machleidt T,

Dahl R, Yuan H, Emdadi A, Barile E, Chen V, Murphy R, Pellecchia M. Design, synthesis, and structure-activity relationship of substrate competitive, selective, and in vivo active triazole and thiadiazole inhibitors of the c-Jun N-terminal kinase. J Med Chem. 2009; 52(7):1943–52. [PubMed: 19271755] (c) De SK, Chen V, Stebbins JL, Chen LH, Cellitti JF, Machleidt T, Barile E, Riel-Mehan M, Dahl R, Yang L, Emdadi A, Murphy R, Pellecchia M. Synthesis and optimization of thiadiazole derivatives as a novel class of substrate competitive c-Jun N-terminal kinase inhibitors. Bioorg Med Chem. 2010; 18(2):590–6. [PubMed: 20045647]

12. (a) Chen T, Kablaoui N, Little J, Timofeevski S, Tschantz WR, Chen P, Feng J, Charlton M, Stanton R, Bauer P. Identification of small-molecule inhibitors of the JIP-JNK interaction. The Biochemical Journal. 2009; 420(2):283–94. [PubMed: 19243309] (b) Comess KM, Sun C, Abad-Zapatero C, Goedken ER, Gum RJ, Borhani DW, Argiriadi M, Groebe DR, Jia Y, Clampit JE, Haasch DL, Smith HT, Wang S, Song D, Coen ML, Cloutier TE, Tang H, Cheng X, Quinn C, Liu B, Xin Z, Liu G, Fry EH, Stoll V, Ng TI, Banach D, Marcotte D, Burns DJ, Calderwood DJ, Hajduk PJ. Discovery and characterization of non-ATP site inhibitors of the mitogen activated protein (MAP) kinases. ACS Chem Biol. 2011; 6(3):234–44. [PubMed: 21090814]
13. Voigt JH, Bienfait B, Wang S, Nicklaus MC. Comparison of the NCI open database with seven large chemical structural databases. J Chem Inf Comput Sci. 2001; 41(3):702–12. [PubMed: 11410049]
14. Fogolari F, Brigo A, Molinari H. Protocol for MM/PBSA molecular dynamics simulations of proteins. Biophys J. 2003; 85(1):159–66. [PubMed: 12829472]
15. Halgren TA, Nachbar RB. Merck molecular force field. IV. conformational energies and geometries for MMFF94. Journal of Computational Chemistry. 1996; 17(5–6):587–615.
16. Middelbeek J, Clark K, Venselaar H, Huynen MA, van Leeuwen FN. The alpha-kinase family: an exceptional branch on the protein kinase tree. Cellular and molecular life sciences : CMLS. 2010; 67(6):875–90. [PubMed: 20012461]
17. Soares KM, Blackmon N, Shun TY, Shinde SN, Takyi HK, Wipf P, Lazo JS, Johnston PA. Profiling the NIH Small Molecule Repository for compounds that generate H2O2 by redox cycling in reducing environments. Assay Drug Dev Technol. 2010; 8(2):152–74. [PubMed: 20070233]
18. Repici M, Mare L, Colombo A, Ploia C, Sclip A, Bonny C, Nicod P, Salmona M, Borsello T. c-Jun N-terminal kinase binding domain-dependent phosphorylation of mitogen-activated protein kinase kinase 4 and mitogen-activated protein kinase kinase 7 and balancing crosstalk between c-Jun N-terminal kinase and extracellular signal-regulated kinase pathways in cortical neurons. Neuroscience. 2009; 159(1):94–103. [PubMed: 19135136]

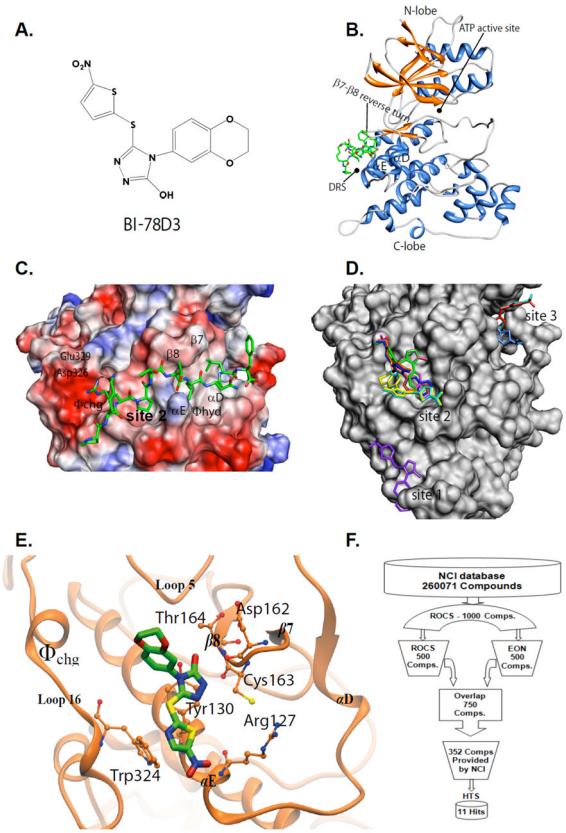

Figure 1.

Ligand Binding to JNK. **A.** Chemical structure of BI-78D3. **B.** Cartoon representation of JNK1 bound to pepJIP1 (amino acids 154–163: PKRPTTLNLF) (PDB ID: 1UKH).[8] **C.** Surface representation of JNK1 bound to pepJIP1. **D.** Molecular docking of BI-78D3 to JNK1. **E.** Determination of the Bioactive Conformation for the Query Ligand BI-78D3 in complex with JNK1 using molecular dynamics. **F.** Schematic representation of the Virtual Screening approaches adopted.

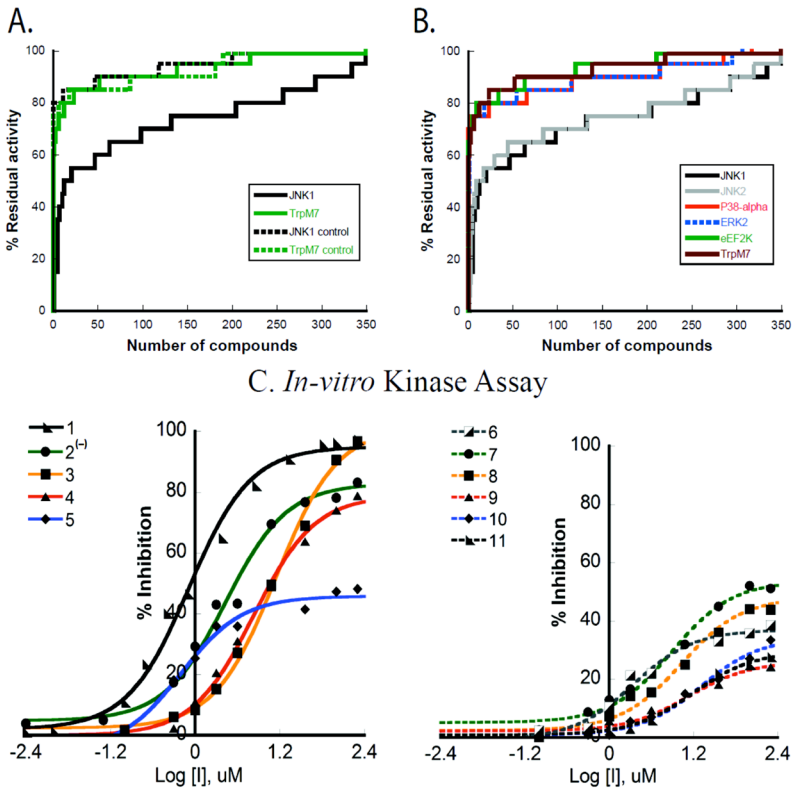

Figure 2.

Assessing the Selectivity of the Virtual Screen. **A.** Comparing the activity of VS-selected (solid line) and randomly selected (dashed line) compounds against JNK1 and TrpM7. **B.** Comparing the activity of VS-selected compounds against indicated kinases. **C**. Inhibition of JNK2 by compounds **1**–**11**.

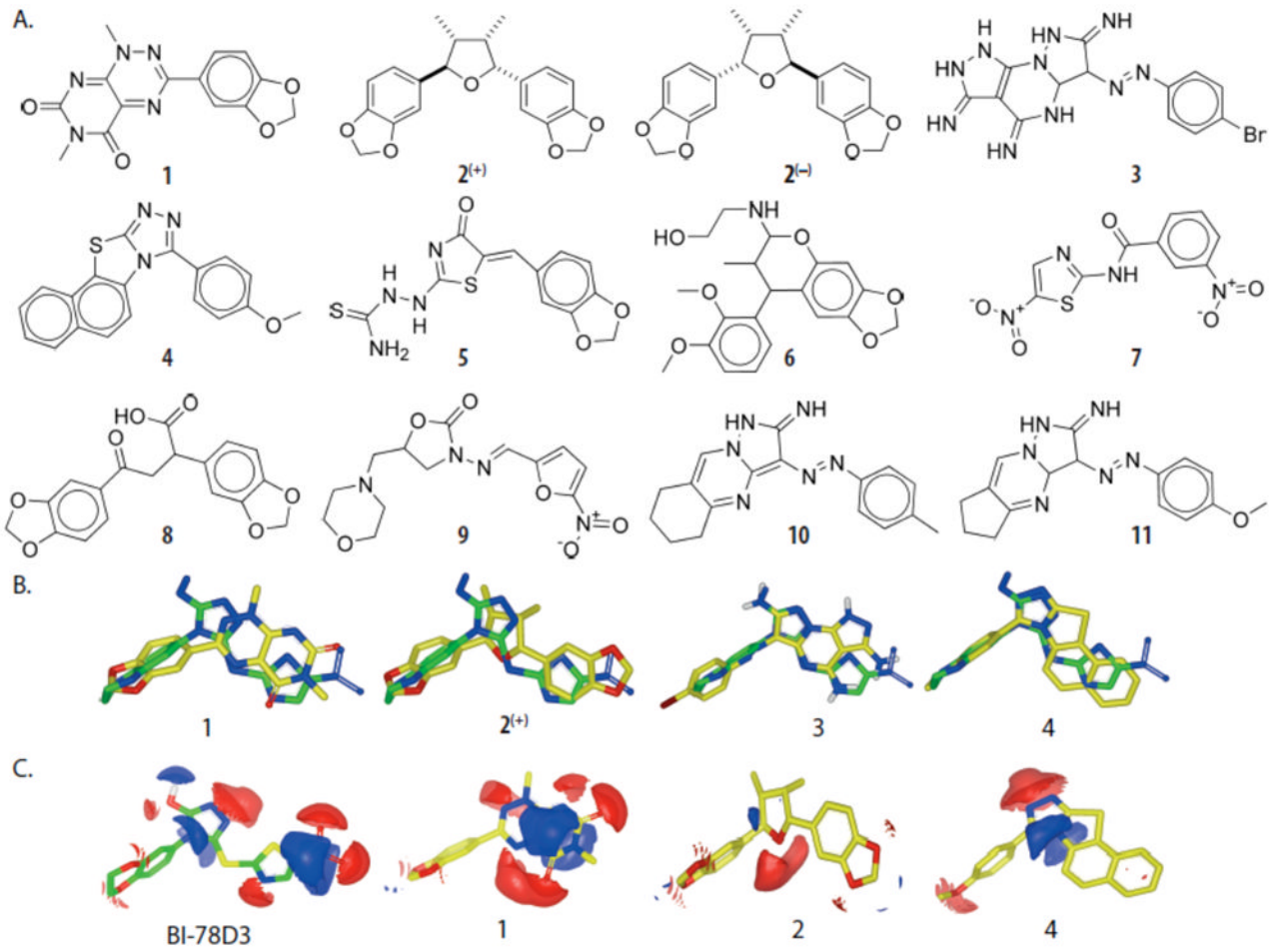

Figure 3.

Top hits identified following biochemical screening. **A.** Chemical Structures of compounds **1** – **11. B.** Overlay of indicated compounds (yellow carbons) and BI-78D3 (green carbons). **C**. Three-dimensional chemical structures of indicated compounds and BI-78D8 with electrostatic surfaces coded by color (red for negative and blue for positive, MMFF94).

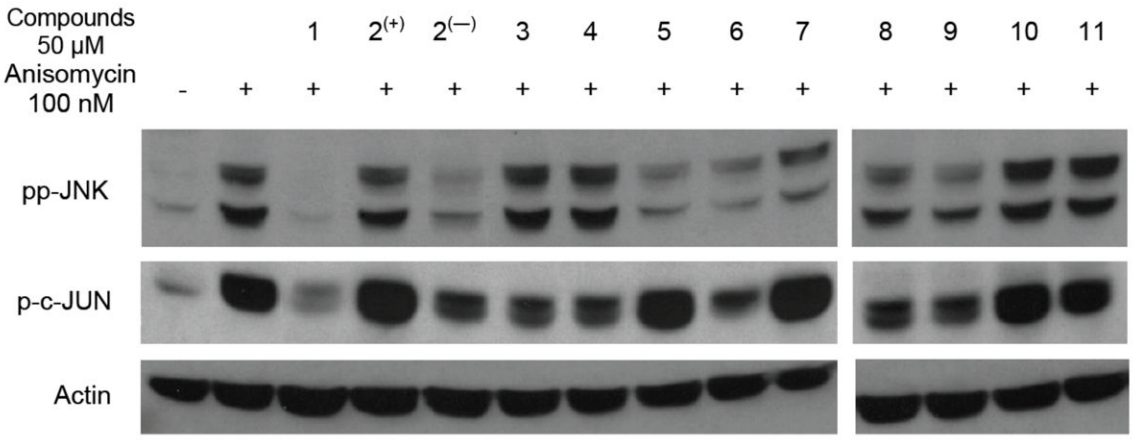

Figure 4.

Cellular Activity. **A.** HEK293 cells were treated with DMSO or 50 μM of the indicated compound for 16 hours then stimulated with anisomycin (50–100 nM) for 5–10 minutes, before lysing the cells and analyzing JNK and c-Jun phosphorylation by Western blotting (one of three representative experiments shown, see Figure S5).[9a]

Table 1

Biochemical analysis of compounds 1–11.

No	JNK2[a]	JNK2[b]	p38MAPKα[a]	ERK2[a]
1	0.7±0.1[c] (100%)	nd[d]	0.5±0.04[c] (50%)	1±0.1[c] (50%)
2(+)	2.5±0.2 (15%)	nd	nd	nd
2(−)	2.5±0.2 (80%)	2.2±0.4 (82%)	252±22 (50%)	295±34 (50%)
3	14±1.3 (100%)	58±6 (100%)	60±10 (57%)	4.6±0.1 (100)
4	21.5±0.9 (80%)	41±6.9 (90%)	2.3±0.2 (24%)	7.5±2 (47%)
5	0.63±0.1 (50%)	1.7±0.16 (50%)	ns[e]	ns
6	2.2±0.16 (40%)	2.2±0.18 (66%)	ns	ns
7	7.7± 1 (53%)	ns	ns	ns
8	10.7±2 (48%)	43±6 (50%)	197±29 (25%)	57±0.6 (45%)
9	13.5±0.7 (20%)	ns	ns	ns
10	20±2.2 (35%)	14.5±1.3 (40%)	ns	ns
11	15.5±3 (30%)	7.8±1 (25%)	ns	ns

[a] kinetic assay,

[b] displacement assay,

[c] determined in the presence of 100 units/mL catalase.

[d] not determined.

[e] not significant.

[f] Values in the table represent IC_{50}, μM and % inhibition at saturation. Dose-response curves for data conforming to inhibition were fitted to: $V_0 = V' - \left(V' \frac{i}{i + (IC_{50})} \right) + V_{00}$ where; V_0 is the observed rate; i is the concentration of inhibitor I; V' is the observed rate in the absence of inhibitor; V_∞ is the observed rate constant at saturating inhibitor, I; IC_{50} is the concentration that leads to half the maximal change in V_0.